

# Consistent Teacher Provides Better Supervision in Semi-supervised Object Detection

Xinjiang Wang<sup>1\*</sup>, Xingyi Yang<sup>1,2,3\*†</sup>, Shilong Zhang<sup>2</sup>, Yijiang Li<sup>1†</sup>, Litong Feng<sup>1</sup>, Shijie Fang<sup>4†</sup>, Chengqi Lyu<sup>2</sup>, Kai Chen<sup>1,2</sup>, and Wayne Zhang<sup>1</sup>

<sup>1</sup> Sensetime Research

<sup>2</sup> Shanghai AI Lab

<sup>3</sup> National University of Singapore

<sup>4</sup> Peking University

wangxinjiang@sensetime.com

**Abstract.** In this study, we dive deep into the unique challenges in semi-supervised object detection (SSOD). We observe that current detectors generally suffer from 3 inconsistency problems. 1) *Assignment inconsistency*, that the conventional assignment policy is sensitive to labeling noise. 2) *Subtasks inconsistency*, where the classification and regression predictions are misaligned at the same feature point. 3) *Temporal inconsistency*, that the pseudo bboxes vary dramatically at different training steps. These issues lead to inconsistent optimization objective of the student network, thus deteriorating performance and slowing down the model convergence. We therefore propose a systematic solution, termed **Consistent-Teacher**, to remedy the above-mentioned challenges. First, adaptive anchor assignment substitutes the static IoU-based strategy, which enables the student network to be resistant to noisy pseudo bboxes; Then we calibrate the subtask predictions by designing a feature alignment module; Lastly, We adopt a Gaussian Mixture Model (GMM) to dynamically adjust the pseudo-boxes threshold. **Consistent-Teacher** provides a new strong baseline on a large range of SSOD evaluations. It achieves 40.0 mAP with ResNet-50 backbone given only 10% of annotated MS-COCO data, which surpasses previous baselines using pseudo labels by around 4 mAP. When trained on fully annotated MS-COCO with additional unlabeled data, the performance further increases to 49.1 mAP. Our code will be open-sourced soon.

**Keywords:** semi-supervised learning, object detection, semi-supervised object detection, anchor assignment

## 1 Introduction

The goal of semi-supervised object detection (SSOD) [18,9,41,17,32,17,51,59] is to facilitate the training of object detectors with the help of a large amount of unlabeled data. The self-training method has been the dominant solution. A teacher

\* Equally contributed.

† Work done during internship at SenseTime.

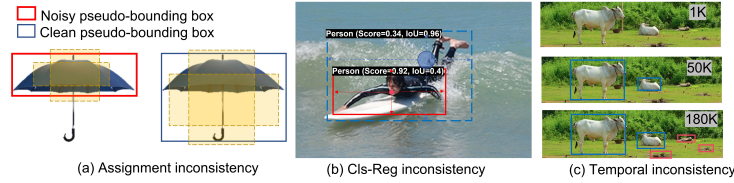


**Fig. 1.** (a). Inconsistent anchors assignment with noisy pseudo-bounding boxes (PB-boxes) based on the static IOU-based assignment methods; (b). The mismatch between high-score (classification) and high-IOU (regression) predictions. The high-score prediction is made from a feature (red dot) in the P4 FPN level whereas the high-IOU prediction is made from a feature (blue dot) in the P5 level; (c). Temporal inconsistency. The change of pseudo-bounding boxes whose scores are higher than a hard threshold 0.5 in RetinaNet at 1K, 50K and 180K training steps. Blue and red boxes denote true positive (TP) and false positive (FP), respectively.

model is first trained to generate pseudo labels and bounding boxes [41] on unlabeled data, which act as the ground truth (GT) for the student model. Student detectors are then anticipated to make similar predictions with the teacher network regardless of network stochasticity [50] or data augmentation [17,41]. In addition, to improve pseudo-label quality, the teacher model is updated as a moving average [32,51,59] of the student parameters.

In this study, we point out 3 fundamental inconsistencies in SSOD that suppress both the performance and convergence speed, namely, Assignment inconsistency, Subtasks inconsistency and Temporal inconsistency. Assignment inconsistency stands for the discrepancy of the training targets caused by the static IOU-based anchor assignment rules. Conventional IOU-based assignment solely relies on the overlapping ratio between anchors and ground truth. Since the pseudo-bounding boxes (PB-boxes) are generated by a stochastically updating teacher model, noises gradually accumulated in box coordinate predictions. As illustrated in Fig. 1(a), even slight distortion in the PB-boxes leads to the substantial anchor assignment shift with naive IOU-based strategy. The assigned label for a specific target may fluctuate between positive and negative during training, which impairs the convergence of the student model.

Subtasks inconsistency refers to the severe misalignment between classification and localization problems in SSOD training. In traditional detectors like Faster R-CNN [37] and RetinaNet [29], the classification and regression tasks are separately predicted and optimized, resulting in the misaligned evaluation for two tasks [47,13,6]. The problem is more manifest in SSOD tasks. As visualized in Figure 1(b), high confidence PB-boxes may not always indicate high-quality box coordinates. Therefore, there are coordinate noises in the generated high-score PB-boxes. The noise would further cause assignment inconsistency and accumulate in SSOD training settings, which is known as confirmation bias [32].

The hard threshold is the third annoying factor that causes temporal inconsistencies in pseudo labels during training. Traditional SSOD methods [41,32,51]

usually adopt a hard threshold on top of the confidence score to distinguish positive PB-boxes from negative ones. However, the hard threshold not only needs to be carefully tuned for each model-task combination but also neglect prediction dynamics the during training. As illustrated in Fig. 1(c), in the MeanTeacher[44] training paradigm, the number of PB-boxes may increase from too few to too many under hard threshold scheme, which incurs biased training for the student. Moreover, this problem is also often intertwined with assignment inconsistency, making training even more difficult.

Therefore, We propose **Consistent-Teacher** in this study to tackle the above issues. First, the static IOU-based anchor assignment is replaced by the adaptive sample assignment (ASA) strategy. During each training step, we calculate the matching cost between each GT (or PB-box) with network predictions. Only feature points with top lowest costs are assigned as positive. The matching cost takes into account the quality of classification and regression. As a result, the dynamic assignment is more resistant to PB-box noises, further enhancing optimization consistency.

Then, we strive to calibrate the classification and regression tasks such that the teacher’s classification confidence also reveals regression quality of each PB-box. The cls-reg alignment problem has been well investigated in traditional object detection settings [13,19,26]. In this study, we propose a 3-D feature alignment module (FAM) to redress the sub-task mismatch problem in SSOD. Specifically, the feature map in the regression sub-branch is re-sampled using a deformable convolution [11] so that the bbox category and coordinate could be adaptively estimated from feature vectors with different locations. Therefore the best feature for regression is ”pulled” to the same position of the best classification feature. Going beyond the 2-D space flexibility, FAM reduce the cls-reg mismatch at various scales by predicting the 3-D offset in the feature pyramid. In this way, a unified confidence score accurately measures the quality of classification and regression with the improved alignment module, and ultimately brings superior supervision for the student in SSOD.

As for the temporal inconsistency in pseudo labels, we apply Gaussian Mixture Model (GMM) to generate an adaptive threshold at training time. Based on the cluster assumption [62] in semi-supervised learning, we consider the confidence scores of each class as a distribution of two modalities of positive or negative samples. We predict the parameters of each Gaussian with maximum likelihood estimation. It is expected that the model is able to adaptively infer the optimal threshold at different training steps. This strategy thus alleviate the need for cumbersome hyperparameter tuning in SSOD, leading to robust improvements under different datasets and settings.

The proposed **Consistent-Teacher** greatly surpasses current SSOD methods. **Consistent-Teacher** reaches 39.8 mAP with 10% of labeled data on MS-COCO, which is 4 mAP ahead of the state-of-the-art [55]. When using the 100% labels together with extra unlabeled MS-COCO data, the performance is further boosted to 49.1 mAP. The effectiveness of **Consistent-Teacher** is also testified

on other ratios of labeled data and on other datasets as well. Concretely, the paper contributes in the following aspects.

- We provides the first in-depth investigation for three inconsistencies in object detection under semi-supervised situation, namely the assignment inconsistency, subtask inconsistency and temporal inconsistency.
- We introduce the adaptive sample assignment to stabilize the matching between noisy PB-boxes and anchors, leading to robust training objective for the student.
- We develop a 3-D task alignment module to calibrate the classification confidence and regression quality, which largely reduces the error in pseudo labels.
- We adopt GMM to flexibly determine the threshold for each class during training. The adaptive threshold evolves through time and reduces the temporal label consistencies for SSOD.
- **Consistent-Teacher** achieves compelling improvement on a wide range of evaluations and serves as a new solid baseline for SSOD.

## 2 Related Work

**Semi-supervised learning.** Semi-supervised learning (SSL) utilizes unlabeled data to improve the model’s performance. Pseudo Label [1,2,39,4,34,54], also known as self-training, works by incorporating the pseudo labels generated on the unlabeled data into training. Recent advancements observed that data consistency [40,49,3], temporal consistency [44] or graph regularization [16,25,33] achieves superior performance by enforcing the averaging model to produce consistent predictions on strongly-augmented or semantically similar input data.

**Semi-supervised object detection (SSOD).** Semi-supervised learning provides a feasible approach to alleviate the labeling cost in object detection problem by learning via a combination of labeled and unlabeled data. A typical framework alternates between training detectors with heuristic consistency constraints [17,42,41] and generating pseudo bounding boxes [32,51,59,27,48,43] for unlabeled images. Student detectors are expected to make consistent prediction on augmented input samples [17,41,53]. [48,51,24] measure the quality of the pseudo labels by quantifying the data uncertainty. [55,32] observed that the imbalanced learning problem in SSOD. In this study, we take a different path and focus on a neglected but fundamental problem in SSOD: noisy pseudo bounding indispose the conventional static anchor assignment rule in object detection. We further design the adaptive anchor assignment strategy that makes anchor assignment invulnerable to noises in bounding boxes generated by the teacher model.

**Hard label assignment in object detection.** Defining positive and negative sample [56] plays a substantial role in object detection. Typical Anchor-based detectors usually adopt hard IoU thresholding as the assigning criterion [37,5,28,29,31,10,36,52]. Conversely, recent center-based anchor-free detectors like YOLOv1 [35], FCOS [45] and Foveabox[22] drop the prior anchor settings and directly define points around the center of objects as positive samples.



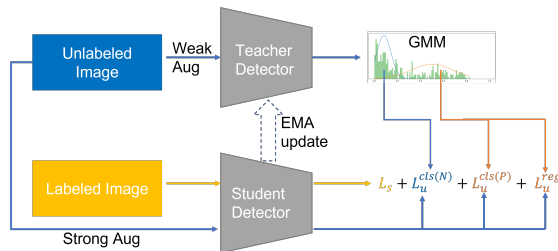


**Fig. 2.** The pipeline of **Consistent-Teacher**. It is based on MeanTeacher where the teacher network is an exponential moving average of the student detector.

Though all detectors mentioned above differ in many aspects, they all adhere to a heuristic hard criteria for assigning labels thus are incapable to adapt to different scenes type and object variations.

**Adaptive anchor assignment.** Going beyond the human-defined criteria, modern detectors have been shifting their focus on learning the label assignment strategy adaptively. To predict shape of object proposals, GuidedAnchoring [46] defines the anchors near the center of ground-truths as positives. FSAF [61] uses the computed loss to select positive samples from feature pyramids. In order to improve the matching between anchors and objects, FreeAnchor [57] and MAL [20] compute the losses to find the best anchor-box. AutoAssign [60] employs automatic label assignment strategy in anchor-free detectors. By fitting the anchor scores distribution, PAA [21] adaptively differentiates the positive anchors and negative ones.

### 3 Consistent-Teacher

In this section, we first provide a quick overview on the semi-supervised detection pipeline. Then we elaborate on our solutions to address the three SSOD inconsistencies, namely Adaptive Sample Assignment, Feature Alignment Module and Gaussian Mixture based thresholding.

#### 3.1 SSOD Detector

We adopt a general SSOD paradigm as our baseline, namely a Mean-Teacher [32,51,44] pipeline with a single-stage object detector, as shown in Fig. 2. The teacher model is maintained as an exponential moving average [44] of a student detector. Unlabeled images first go through weak augmentations and are then input into the teacher detector to generate pseudo bboxes. These pseudo bboxes are then provided as the supervision for the student network, where the same unlabeled image are strongly jittered. In this way, the network can implicitly learn an invariant embedding across different views and thus leverage large amount of unlabeled images to increase the performance. In the meantime, a small set of labeled images are also fed into the student detector to learn discriminative

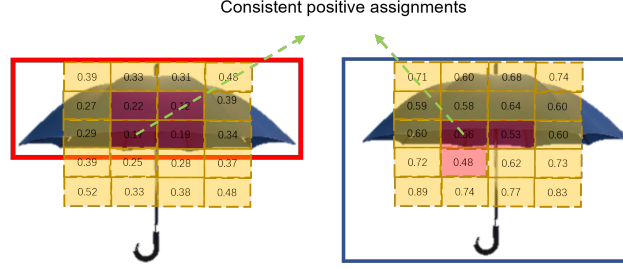


**Fig. 3.** The assignment results for different PB-bboxes in ConsistentTeacher according to Eq. 2, The rectangles filled with yellow and red represents positive and negative feature points, respectively. The number inside each rectangle denotes its matching cost.

representation for both classification and regression. The goal of the student network is to minimize the loss

$$\mathcal{L} = \mathcal{L}_s + \lambda_u(\mathcal{L}_u^{cls} + \lambda^{reg}\mathcal{L}_u^{reg}), \quad (1)$$

where  $\mathcal{L}_s$  and  $\mathcal{L}_u$  denote supervised and unsupervised (unlabeled) losses, respectively.  $\lambda_u$  is the loss weight for  $\mathcal{L}_u$  and  $\lambda^{reg}$  is the loss weight for the regression subtask. In this study, we primarily concentrate on SSOD with single-stage detectors, e.g. RetinaNet [29], since it is more easily implemented and already achieves a competitive performance [58].

### 3.2 Consistent and Adaptive Sample Assignment.

Each anchor in RetinaNet is assigned as positive only if its IOU with ground truth (gt) bbox is larger than a certain threshold. As described in Sec. 1, the static IOU-based assignment strategy is not robust with noise in pseudo bboxes. Therefore, we propose to adopt an Adaptive Sample Assignment (ASA) strategy. Specifically, a matching cost between each prediction and given ground-truth (also including pseudo bboxes) is calculated [14,15,7] and the assignment is executed according to the relative matching cost. Given a feature point  $p_i$ , the detector gets its predicted bbox  $\text{Pred}(p_i)$ . The cost between each gt  $b_i$  and the prediction from a feature point  $p_j$  is calculated as

$$C_{ij} = \lambda_{cls}C_{cls} + \lambda_{reg}C_{reg} + \lambda_{dist}C_{dist}, \quad (2)$$

$$\text{where } C_{cls} = L_{cls}(\text{Pred}(p_i)_{cls}, b_i) \quad (3)$$

$$C_{reg} = L_{reg}(\text{Pred}(p_i)_{reg}, b_i) \quad (4)$$

$$C_{dist}(i, j) = 10^{\|d(p_j, b_i)\|_2} \quad (5)$$

where  $C_{cls}$  and  $C_{reg}$  denote the classification and regression costs and are chosen as the classification and regression losses respectively.  $C_{dist}(i, j)$  measures

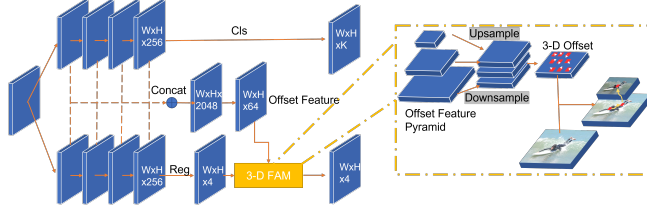


**Fig. 4.** The detector head structure of ConsistentTeacher. The left part is the head structure and the right part denotes the 3D FAM module.

the center prior, where  $\|\mathbf{d}(p_j, b_i)\|_2$  is the distance of feature point  $p_j$  to the center of  $b_i$ , normalized by the striding step in the FPN level.  $\lambda_{cls}$ ,  $\lambda_{reg}$  and  $\lambda_{dist}$  are weighting parameters. After sorting out the matching cost between  $b_i$  with all feature points  $p_j$ , feature points of top  $K$  lost costs are viewed as positive candidates. It should be noted that  $C_{dist}$  mainly stabilize the assignment especially at the beginning of training and  $\lambda_{dist} \sim 0.001$  is a small number. Therefore, the matching cost is still dominated by the classification and regression qualities. Since the assignment is made in accordance with detection quality, noise in pseudo-bboxes would have a negligible impact on feature points assignment. Therefore, the optimization target would be more consistent with the existence of noisy pseudo bboxes, as seen in Fig. 3.

### 3.3 Consistent Sub-task Predictions with 3-D Feature Alignment.

In SSOD, we observe severe misalignment between the best cls-reg predictions using the same feature point, which results in less calibrated regression quality according to the confidence scores. Therefore, we introduce a 3-D Feature Alignment Module (3D-FAM) to adaptively select different feature locations to accomplish each sub-task.

3D-FAM estimates the offset of optimal the regression feature points so that they are better aligned with the output of the classification branch, inspired by TOOD [13]. While the offset is confined to 2-D space in TOOD, *i.e.*, at the same feature scale level, We extend the offset to 3-D space so that feature points are able to be offset to different FPN levels and different scales as well. In our implementation, the offset prediction module is realized via a sub-branch in the head structure that predict the offset of the decoded bbox coordinates in 3-D dimensions. As illustrated in Fig. 4(a), apart from the parallel branches for cls and reg subtasks, we add an extra branch with input of the concatenated intermediate layers of both cls and reg branches. The concatenated feature map  $f \in \mathcal{R}^{H \times W \times 8C}$ , where  $C = 256$  is the channel number of intermediate features. A  $1 \times 1$  conv follows the concatenation to reduce the dimension to  $f' \in \mathcal{R}^{H \times W \times C/4}$ , the feature  $f'$  is then kept in each FPN level to predict a 3-D offset. The 3-D offset prediction architecture is shown in Fig. 4(b). Then  $f'_{l-1}$  and  $f'_{l+1}$  are interpolated to the same size as  $f'_l$ , where  $l$  is the index of FPN level. Features across different FPN layers are concatenated to output the offset prediction

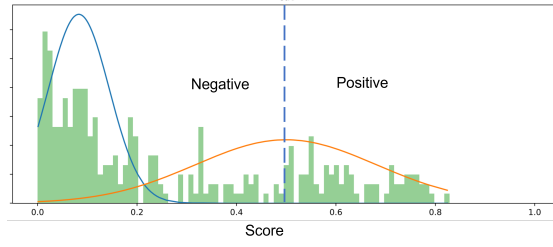


**Fig. 5.** The score distribution and the fitted results of two Gaussian mixtures. The positive and negative distributions are in orange and blue lines, respectively. The blue dash line denotes the final threshold.

$O \in \mathcal{R}^{H \times W \times 12}$ , which enables each boundary prediction feature point  $P(i, j, l)$  to find their individual offset, where  $0 < i \leq H, 0 < j \leq W$  are position indices, and  $l$  indexes the FPN level. Each offset is in 3-D space and is denoted as  $\mathbf{d} = (d_1, d_2, d_3)$ , where  $d_1(i, j, l) = O(i, j, 3c + 1)$ ,  $d_2(i, j, l) = O(i, j, 3c + 2)$  and  $d_3 = O(i, j, 3c + 3)$ . The offset process is executed in two consecutive steps,

$$P^h(i, j, l) \leftarrow P(i + d_1, j + d_2, l) \quad (6)$$

$$P^{out}(i, j, l) \leftarrow P^h(i/2^{d_3}, j/2^{d_3}, l + d_3), \quad (7)$$

where Eq. 6 is to conduct offset in a 2-D space and Eq. 7 is the offset across different FPN levels and is realized by bilinear interpolation. As for the bottom and top levels, the offset  $d_3$  is clipped to ensure meaningful coordinate output.

### 3.4 Temporal consistency using Gaussian Mixture Model (GMM)

Previous works [41,32] require a preset hyperparameter  $\tau$  for selecting pseudo bboxes. However, it has to be carefully tuned on various datasets. Furthermore, applying a fixed threshold ignores the fact that the model’s prediction confidence varies across categories and iterations.

To overcome these limitations, we want to discriminate positive and negative pseudo bboxes with a rule of probability. Specifically, we assume that the confidence scores are drawn from a mixture of Gaussian distributions.

$$P(b|s, \theta) = w_n \mathcal{N}_n(b, \mu_n, p_n) + w_p \mathcal{N}_p(b, \mu_p, p_p), \quad (8)$$

where  $b$  is the confidence score of a pseudo bbox,  $w_n, \mu_n, p_n$  and  $w_p, \mu_p, p_p$  represent the weight, mean and precision of two Gaussians, respectively. For each category, we maintain a confidence score bank of size  $N$  used to optimize the GMM with Expectation-Maximization (EM) algorithm at each step. After the parameters of GMM have been obtained, the probability of each pseudo bbox being positive or negative can be determined. The threshold  $\tau$  is determined by the sample with the highest probability to be positive as shown in Fig. 5:

$$\tau = \arg \max_b P_{pos}(b|s, \theta) \quad (9)$$

The model’s learning status can be represented by the distribution of confidence scores. By using the latest  $N$  samples for fitting GMM, the threshold can be adaptively adjusted w.r.t. the model’s performance at present. Furthermore, since the parameters of GMM are optimized separately for each category, the thresholds of the different categories can be dynamically computed. Difficult categories, for example, have lower thresholds due to the low confidence scores of most pseudo bboxes.

## 4 Experiments

**Datasets and Evaluation Setup.** To validate the performance of our proposed **Consistent-Teacher**, we conduct comprehensive experiment on the MS-COCO [30] benchmark and PASCAL VOC datasets [12].

We includes three evaluation protocols: (1) COCO-PARTIAL: We randomly sample 1%/2%/5%/10% of the images in **train2017** as labeled data and treat the rest as unlabeled data. We report the  $AP_{50:95}$  results on the **val2017** as the evaluation metrics. (2) COCO-ADDITION: We use the full **train2017** as labeled set and includes coco official unlabeled set **unlabel2017** as unlabeled set. The trained model are evaluated on **val2017**. (3) VOC-PARTIAL: We utilize the VOC2007 trainval set as the labeled data and make use of the VOC2012 trainval as our unlabeled data. The final model is verified on VOC2007 test set using  $AP_{50}$  and  $AP_{50:95}$ .

**Implementation Details.** To ensure a fair comparison, all detectors are trained on 8 GPUs with 5 images per GPU (1 labeled and 4 unlabeled images). The detectors are optimized using SGD with a constant learning rate of 0.01, momentum of 0.9 and weight decay of 0.001. The unlabeled data weight is  $\lambda_U = 2$ . No learning rate decay is applied. In COCO-PARTIAL and VOC-PARTIAL evaluation, we train the detectors for 180K iterations, whereas we double the training time on COCO-ADDITION to 360K for better convergence. The teacher model is updated through EMA with a momentum of 0.999. We follow the same data preprocessing and augmentation pipeline in [51] without modifications. We set RetinaNet as our default detection framework and use the ResNet-50-FPN [28] as its backbone. ImageNet-pretrained model is used as initialization.

We compare our **Consistent-Teacher** with numerous prevailing SSOD approaches including CSD [17], STAC [41], Instant Teaching [59], Humble Teacher [43], Unbiased Teacher [32], Soft Teacher [51], ACRST [55], DSL [8], S4OD [58] and PseCo [23]. In addition, we implement a baseline method where students are trained using labeled and pseudo-labeled data, and the teacher is updated through EMA of student. We name it the Mean-Teacher baseline [44]. The default confidence threshold is set as 0.4.

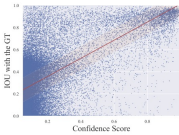
### 4.1 Revisiting the Inconsistency Problems in SSOD

To further justify the existence of inconsistency in SSOD, we provide analytic and quantitative evidence for the *Assignment Inconsistency*, *Subtasks Inconsistency* and *Temporal Inconsistency* respectively.

**Assignment Inconsistency under Noisy Pseudo Labels.** To illustrate that the conventional IOU-based or heuristic label assignment is problematic in SSOD, we intentionally inject random noise to the ground-truth bounding boxes and testify the assignment consistency by quantifying the assignment IOU (A-IOU) between clean and noisy assignments. Suppose a bounding box  $b = (x_1, y_1, x_2, y_2)$  is assigned to a set of  $k$  anchors  $A = \{a_1, \dots, a_k\}$ . We add Gaussian noise to its coordinate with a noise ratio  $\rho$ , so that  $b' = (x_1 + \epsilon_{x_1} \times w, y_1 + \epsilon_{y_1} \times h, x_2 + \epsilon_{x_2} \times w, y_2 + \epsilon_{y_2} \times h)$ , in which  $w$  and  $h$  are width and height of the box.  $\epsilon_{x_1}, \epsilon_{y_1}, \epsilon_{x_2}, \epsilon_{y_2}$  are sampled from a normal distribution  $\mathcal{N}(0, \rho)$ . The perturbed box  $b'$  is matched to a new set of  $l$  anchors  $A' = \{a'_1, \dots, a'_l\}$ . The A-IOU is computed as the intersection-of-union between  $A$  and  $A'$ . The higher A-IOU score suggests the assignment is more robust to label noise.

We testify the assignment consistency under two scenario. First, we calculate the assignment IOU with different degrees of noise ratio  $\rho \in \{0.1, 0.2, \dots, 0.5\}$  using the final model. Second, we would like to investigate how the assignment consistency change through training. We report the A-IOU at different time of training with a constant  $\rho = 0.1$ . We compare our ASA with IOU-based assigner [37,29,31] and ATSS assigner [56] with Mean Teacher RetinaNet baseline on COCO 10%. All modules except for the assignment are kept the same to provide a fair comparison. For both evaluations, we randomly select 1000 images from val2017 to compute the A-IOU. Figure 6 visualize the mean $\pm$ std A-IOU between clean label and noisy bounding boxes at different training time and different noise ratio  $\rho$ . In Figure 6(a), both ATSS assign and our ASA provides higher A-IOU compared with the broadly applied IOU-based assignment scheme. However, ATSS is still based on heuristic matching rule between label and anchor boxes. ASA, instead, steadily improves itself as the detector becomes more accurate. In Figure 6(b), we see that IOU-based assignment fails to maintain the initial assignment when the large magnitude of noise is introduced in the labels. Given the noisy nature of pseudo label in SSOD, our experiment suggests that IOU-based assignment is incapable to maintain the assignment consistency in SSOD. In contrast, our ASA strategy still outperformed its competitors under server noise scenario. It supports our argument our Consistent assignment strategy is robust to label noise in SSOD.

**Table 1.** Classification and Regression inconsistency analysis using IOU-Confidence linear regression (LR) error. We also provide the Mean Teacher IOU-Confidence plot on the right.

	LR Standard Error	
Mean Teacher	0.109	
Consistent-Teacher	<b>0.080</b>	

**Classification and Regression Inconsistency.** We unveil the regression and classification mismatch problem in SSOD by identifying the mismatch between

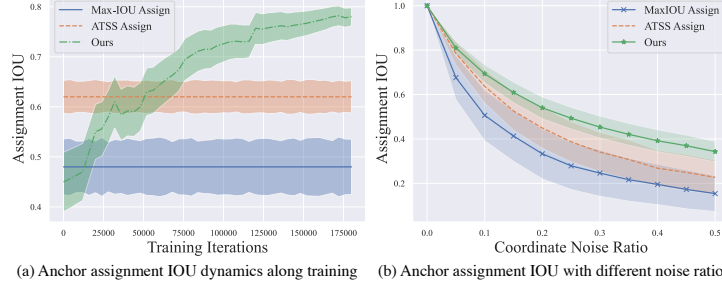


**Fig. 6.** Assignment IOU score between ground-truth and the noisy bounding boxes (a) at different time of training and (b) using different noise ratio.

the high-score and high-IOU predictions. We obtain the confidence-IOU pairs on val2017 using **Consistent-Teacher** and Mean Teacher RetinaNet when trained on COCO 10% data, and analyze the correlation between the two variables. We apply linear regression and measures the standard error to reflect the correlation between confidences and IOUs. Smaller error indicates higher correlation.

Table 1 provides the LR standard error for **Consistent-Teacher** and Mean Teacher RetinaNet. The right figure demonstrates the confidence-IOU scatter for Mean Teacher. We observe clear cls-reg misalignment on semi-supervised detectors: A lot of low-confident prediction actually has high IOU score with the ground-truth label. It indicates classification confidence does not provides strong clue for accurate regression results, which give arise to erroneous pseudo-label results during training. Mean teacher therefore has a high LR error with 0.109. On the contrary, our **Consistent-Teacher** largely diminishes the mismatch between two tasks, end up with a lower error of 0.080. It supports our arguments that **Consistent-Teacher** is able to align the cls-reg mismatch in SSOD.

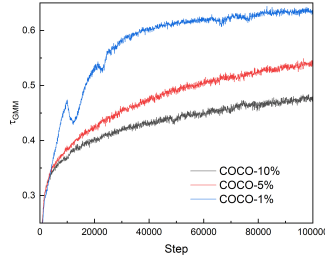


**Fig. 7.** GMM threshold dynamics along training.

**Temporal Inconsistency.** In this paragraph, we address the necessity of adaptive confidence threshold during training. We plot the best threshold curve obtained by GMM on COCO 1%/5%/10% training in Figure 7. An evident trend exists in SSOD that, as the detector becomes more accurate, the GMM threshold also steadily increase as training proceeds. In addition, the confident threshold should also be uplifted according to the number of the labeled data. Based on above-mentioned temporal inconsistency, typical static threshold setting is inca-

**Table 2.** COCO-PARTIAL comparison with other semi-supervised detector on val2017. All results are the average of 5 folds. We also report the Faster-RCNN performance trained on labeled data only. All models adopt ResNet50 with FPN as backbone. † denotes structure modification referred in Sec. 3.3.

Method	Detector	1% COCO	2% COCO	5% COCO	10% COCO
Labeled Only	FRCNN	9.05±0.16	12.70±0.15	18.47±0.22	23.86±0.81
CSD	FRCNN	10.51±0.06	13.93±0.12	18.63±0.07	22.46±0.08
STAC	FRCNN	13.97±0.35	18.25±0.25	24.38±0.12	28.64±0.21
Instant Teaching	FRCNN	18.05±0.15	22.45±0.15	26.75±0.05	30.40±0.05
Humble teacher	FRCNN	16.96±0.38	21.72±0.24	27.70±0.15	31.61±0.28
Unbiased Teacher	FRCNN	20.75±0.12	24.30±0.07	28.27±0.11	31.50±0.10
Soft Teacher	FRCNN	20.46±0.39	-	30.74±0.08	34.04±0.14
ACRST	FRCNN	26.07±0.46	28.69±0.17	31.35±0.13	34.92±0.22
PseCo	FRCNN	22.43±0.36	27.77±0.18	32.50±0.08	36.06±0.24
Labeled Only	RetinaNet	7.40±0.23	11.00±0.26	17.20±0.18	21.00±0.22
S4OD	RetinaNet	20.10±0.12	-	30.00±0.21	32.90±0.11
DSL	FCOS	22.03±0.28	25.19±0.37	30.87±0.24	36.22±0.18
Mean-Teacher	RetinaNet	20.40±0.28	26.00±0.18	30.40±0.15	35.50±0.08
<b>Consistent-Teacher</b>	RetinaNet <sup>†</sup>	<b>26.30±0.32</b>	<b>31.20±0.21</b>	<b>35.70±0.14</b>	<b>40.00±0.13</b>

pable to filter out superior pseudo-label boxes, while GMM provides a gratifying solution.

## 4.2 Semi-supervised Object Detection

In this section, we compare our method with previous state-of-the-arts under COCO-PARTIAL, VOC-PARTIAL and COCO-ADDITION evaluation protocol.

**COCO-partial Results.** Table 2 systematically compares  $AP_{50:95}$  of all aforementioned semi-supervised detectors trained with COCO 1%/2%/5%/10% labels. We first note that the simple Mean Teacher baseline with RetinaNet detector constitutes a strong method for SSOD. It achieves an  $AP_{50:95}$  of 35.5 on COCO 10% experiments without sophisticated data re-weighting strategy or pseudo labeling selection methods [51]. More surprisingly, Consistent-Teacher achieves remarkable progress over current methods. It scores 40.00  $AP_{50:95}$  on COCO 10% data, largely surpassing the best-performed model by  $\sim 4 AP_{50:95}$ .

**Table 3.** VOC-PARTIAL experimental results comparison with other semi-supervised detector on VOC2007 test. All models adopt ResNet50-FPN as backbone.

Method	Detector	Labeled	Unlabeled	$AP_{50}$	$AP_{50:95}$
Labeled Only	FRCNN	VOC07	-	72.63	42.13
Labeled Only	RetinaNet	VOC07	-	73.23	44.08
CSD	FRCNN	VOC07	VOC12	74.70	-
STAC	FRCNN	VOC07	VOC12	77.45	44.64
Unbiased Teacher	FRCNN	VOC07	VOC12	77.37	48.69
ACRST	FRCNN	VOC07	VOC12	78.16	50.12
Mean-Teacher	RetinaNet	VOC07	VOC12	77.02	53.61
<b>Consistent-Teacher</b>	RetinaNet	VOC07	VOC12	<b>80.64</b>	<b>58.01</b>



**VOC-partial Results.** In addition to the COCO evaluations, we compare our proposed model against other SSOD approaches on VOC0712 datasets in Table 3. Again, we notice that our **Consistent-Teacher** makes outstanding improvements over its counterparts. Our method shows an improvement of 7.9 absolute mAP compared with the latest state-of-the-art.

**COCO-addition Results.** Now we would like to push our model to its limits by taking the full COCO train **train2017** as labeled data and additional **unlabel2017** as unlabeled data. As shown in Table 4, in the case of COCO-ADDITION, our model trained for 360K iterations achieves 49.10  $AP_{50:95}$  using ResNet-50 as backbone. Compared with the current state-of-the-art semi-supervised detectors such as PseCo, **Consistent-Teacher** achieves 3.0  $AP_{50:95}$  promotion even with only  $\frac{1}{2}$  training time.

**Table 4.** COCO-ADDITION experimental results on **val2017** with **unlabel2017** as unlabeled set. Note that 1 $\times$  represents 90K training iterations, and N $\times$  represents N $\times$ 90K training iterations.

Method	$AP_{50:95}$
Supervised(3 $\times$ )	40.20
Supervised(3 $\times$ )	39.50
CSD(3 $\times$ )	38.82
STAC(6 $\times$ )	39.21
Unbiased Teacher(3 $\times$ )	41.30
ACRST(3 $\times$ )	42.79
Soft Teacher(16 $\times$ )	44.50
DSL(2 $\times$ )	43.80
PseCo(8 $\times$ )	46.10
MeanTeacher-RetinaNet(4 $\times$ )	40.78
<b>Consistent-Teacher</b> (4 $\times$ )	<b>49.10</b>

### 4.3 Ablation Study

In this section, we validate the effectiveness of our 3 major designs on the COCO 10% setting.

**Adaptive Sample Assignment.** We first examine the effect of ASA strategy. To enable a fair comparison between all assigners, we utilize the Mean Teacher with fixed confidence threshold 0.4 and unlabeled weight of 2 as our baseline and

replace its IOU-based assignment with our proposed ASA. It is notable that, as shown in Table 5, robust sample assignment plays a pivotal role in SSOD. By specializing the assignment policy on semi-supervised tasks, our ASA achieves 38.50  $AP_{50:95}$  on COCO 10%.

**Feature Alignment Module.** To testify the effectiveness of FAM, we first replace the 3-D FAM as a 2-D counterpart, which is adopted in [13]. Table 6 provides the ablative study of our method with different head structure. We observe that the 3-D FAM surpasses the setting without feature alignment by

**Table 5.** Comparisons between different schemes of training sample assignments on COCO 10% evaluation.

Assignment	$AP_{50:95}$
IOU-based	35.50
our ASA	<b>38.50</b>

1.1 mAP and 2-D FAM by 0.5 mAP on COCO 10% evaluation, with negligible parameters and FLOPs. It is shown that, by automatically estimating the best 3D feature location for classification and regression, the semi-supervised detector are better calibrated to identify high quality pseudo-labels.

**Table 6.** Ablation Study on detection head structure. We compare the performance, Model size and FLOPs on different head structures on COCO 10%. FLOPs are measured on the input image size of  $1280 \times 800$ .

Method	Head/full Params (M)	Head/full FLOPs (G)	$AP_{50:95}$
Consistent-Teacher w/o FAM	4.92/32.07	104.87/205.21	38.90
Consistent-Teacher w 2-D FAM	4.94/32.04	105.36/205.70	39.50
Consistent-Teacher w 3-D FAM	5.07/32.22	108.15/208.49	<b>40.00</b>

**GMM.** We testify the detector performance with or without the GMM-based pseudo-labelling. We replace it with a hard confidence threshold  $\tau \in (0.2, 0.3, 0.4, 0.5, 0.6, 0.9)$ . Table 7 illustrates the test mAP on *val2017*. Notice that the confidence threshold is a sensitive parameter, with the optimal constant threshold at 0.4. By fitting the distribution of confidence, GMM dynamically adjusts the threshold for selecting pseudo-labels. This allows our model to gain more accuracy supervision signal than a fixed threshold, achieving the final performance of 40.00  $AP_{50:95}$  with 0.5 mAP improvement on 10% labeled data. GMM is also higher than the model using hard threshold (0.4) at different ratios of labeled data as well, as illustrated in Table 8.

**Table 7.** Ablative study of GMM-based pseudo-label filtering. Each value represents the  $AP_{50:95}$  on COCO 10% data.

threshold $\tau$	0.2	0.3	0.4	0.5	0.6	0.9
Consistent-Teacher w/o GMM	37.1	39.1	39.5	38.4	34.9	31.6
Consistent-Teacher	<b>40.0</b>					

**Table 8.** Ablation of GMM at different labeled data ratio on COCO. Models are compared to baselines with a hard threshold 0.4.

threshold	1%	2%	5%	10%	FULL
Consistent-Teacher w/o GMM	25.0	30.5	36.3	39.5	48.7
Consistent-Teacher w/ GMM	<b>26.3</b> <sub>(+1.3)</sub>	<b>31.2</b> <sub>(+0.7)</sub>	<b>36.7</b> <sub>(+0.4)</sub>	<b>40.0</b> <sub>(+0.5)</sub>	<b>49.1</b> <sub>(+0.4)</sub>

## 5 Conclusion and Future work

In this paper, we systematically investigate three types of the inconsistency problems in semi-supervised object detection, namely, assignment inconsistency, cls-reg sub-task inconsistency and temporal inconsistency. To alleviate the aforementioned problem, we present a simple yet effective semi-supervised object detector termed **Consistent-Teacher**. In **Consistent-Teacher**, we introduce

Consistent anchor assignment which selects the top-K matching with lowest costs and FAM which regress the 3-D feature pyramid offsets that aligns classification and regression tasks. To solve the temporal inconsistency in PB-boxes, we leverage GMM to dynamically adjust the threshold for self-training. Though integration of three designs, our **Consistent-Teacher** is able to simultaneously obtain a robust anchor assignment with consistent PB-boxes outperforming the state-of-the-art methods by a large margin on a series of SSOD benchmarks.

## References

1. Pseudo-label: The simple and efficient semi-supervised learning method for deep neural networks. In: Workshop on challenges in representation learning, ICML. vol. 3, p. 896 (2013)
2. Arazo, E., Ortego, D., Albert, P., O'Connor, N.E., McGuinness, K.: Pseudo-labeling and confirmation bias in deep semi-supervised learning. In: 2020 International Joint Conference on Neural Networks (IJCNN). pp. 1–8. IEEE (2020)
3. Berthelot, D., Carlini, N., Goodfellow, I., Papernot, N., Oliver, A., Raffel, C.: Mixmatch: A holistic approach to semi-supervised learning. arXiv preprint arXiv:1905.02249 (2019)
4. Blum, A., Mitchell, T.: Combining labeled and unlabeled data with co-training. In: Proceedings of the eleventh annual conference on Computational learning theory. pp. 92–100 (1998)
5. Cai, Z., Vasconcelos, N.: Cascade r-cnn: Delving into high quality object detection. In: Proceedings of the IEEE conference on computer vision and pattern recognition. pp. 6154–6162 (2018)
6. Cao, Y., Chen, K., Loy, C.C., Lin, D.: Prime sample attention in object detection. In: Proceedings of the IEEE/CVF Conference on Computer Vision and Pattern Recognition. pp. 11583–11591 (2020)
7. Carion, N., Massa, F., Synnaeve, G., Usunier, N., Kirillov, A., Zagoruyko, S.: End-to-end object detection with transformers. In: European conference on computer vision. pp. 213–229. Springer (2020)
8. Chen, B., Li, P., Chen, X., Wang, B., Zhang, L., Hua, X.S.: Dense learning based semi-supervised object detection. In: Proceedings of the IEEE/CVF Conference on Computer Vision and Pattern Recognition. pp. 4815–4824 (2022)
9. Chen, C., Dong, S., Tian, Y., Cao, K., Liu, L., Guo, Y.: Temporal self-ensembling teacher for semi-supervised object detection. IEEE Transactions on Multimedia (2021)
10. Dai, J., Li, Y., He, K., Sun, J.: R-fcn: Object detection via region-based fully convolutional networks. Advances in neural information processing systems **29** (2016)
11. Dai, J., Qi, H., Xiong, Y., Li, Y., Zhang, G., Hu, H., Wei, Y.: Deformable convolutional networks. In: Proceedings of the IEEE international conference on computer vision. pp. 764–773 (2017)
12. Everingham, M., Van Gool, L., Williams, C.K.I., Winn, J., Zisserman, A.: The PASCAL Visual Object Classes Challenge 2012 (VOC2012) Results. <http://www.pascal-network.org/challenges/VOC/voc2012/workshop/index.html>
13. Feng, C., Zhong, Y., Gao, Y., Scott, M.R., Huang, W.: Tood: Task-aligned one-stage object detection. In: Proceedings of the IEEE/CVF International Conference on Computer Vision. pp. 3510–3519 (2021)
14. Ge, Z., Liu, S., Li, Z., Yoshie, O., Sun, J.: Ota: Optimal transport assignment for object detection. In: Proceedings of the IEEE/CVF Conference on Computer Vision and Pattern Recognition. pp. 303–312 (2021)
15. Ge, Z., Liu, S., Wang, F., Li, Z., Sun, J.: Yolox: Exceeding yolo series in 2021. arXiv preprint arXiv:2107.08430 (2021)
16. Iscen, A., Tolias, G., Avrithis, Y., Chum, O.: Label propagation for deep semi-supervised learning. In: Proceedings of the IEEE/CVF Conference on Computer Vision and Pattern Recognition. pp. 5070–5079 (2019)

17. Jeong, J., Lee, S., Kim, J., Kwak, N.: Consistency-based semi-supervised learning for object detection. *Advances in neural information processing systems* **32** (2019)
18. Jeong, J., Verma, V., Hyun, M., Kannala, J., Kwak, N.: Interpolation-based semi-supervised learning for object detection. In: *Proceedings of the IEEE/CVF Conference on Computer Vision and Pattern Recognition*. pp. 11602–11611 (2021)
19. Jiang, B., Luo, R., Mao, J., Xiao, T., Jiang, Y.: Acquisition of localization confidence for accurate object detection. In: *Proceedings of the European conference on computer vision (ECCV)*. pp. 784–799 (2018)
20. Ke, W., Zhang, T., Huang, Z., Ye, Q., Liu, J., Huang, D.: Multiple anchor learning for visual object detection. In: *Proceedings of the IEEE/CVF Conference on Computer Vision and Pattern Recognition*. pp. 10206–10215 (2020)
21. Kim, K., Lee, H.S.: Probabilistic anchor assignment with iou prediction for object detection. In: *European Conference on Computer Vision*. pp. 355–371. Springer (2020)
22. Kong, T., Sun, F., Liu, H., Jiang, Y., Li, L., Shi, J.: Foveabox: Beyond anchor-based object detection. *IEEE Transactions on Image Processing* **29**, 7389–7398 (2020)
23. Li, G., Li, X., Wang, Y., Zhang, S., Wu, Y., Liang, D.: Pseco: Pseudo labeling and consistency training for semi-supervised object detection. *arXiv preprint arXiv:2203.16317* (2022)
24. Li, H., Wu, Z., Shrivastava, A., Davis, L.S.: Rethinking pseudo labels for semi-supervised object detection. *arXiv preprint arXiv:2106.00168* (2021)
25. Li, J., Xiong, C., Hoi, S.C.: Comatch: Semi-supervised learning with contrastive graph regularization. In: *Proceedings of the IEEE/CVF International Conference on Computer Vision*. pp. 9475–9484 (2021)
26. Li, X., Wang, W., Wu, L., Chen, S., Hu, X., Li, J., Tang, J., Yang, J.: Generalized focal loss: Learning qualified and distributed bounding boxes for dense object detection. *Advances in Neural Information Processing Systems* **33**, 21002–21012 (2020)
27. Li, Y., Huang, D., Qin, D., Wang, L., Gong, B.: Improving object detection with selective self-supervised self-training. In: *European Conference on Computer Vision*. pp. 589–607. Springer (2020)
28. Lin, T.Y., Dollár, P., Girshick, R., He, K., Hariharan, B., Belongie, S.: Feature pyramid networks for object detection. In: *Proceedings of the IEEE conference on computer vision and pattern recognition*. pp. 2117–2125 (2017)
29. Lin, T.Y., Goyal, P., Girshick, R., He, K., Dollár, P.: Focal loss for dense object detection. In: *Proceedings of the IEEE international conference on computer vision*. pp. 2980–2988 (2017)
30. Lin, T.Y., Maire, M., Belongie, S., Hays, J., Perona, P., Ramanan, D., Dollár, P., Zitnick, C.L.: Microsoft coco: Common objects in context. In: *European conference on computer vision*. pp. 740–755. Springer (2014)
31. Liu, W., Anguelov, D., Erhan, D., Szegedy, C., Reed, S., Fu, C.Y., Berg, A.C.: Ssd: Single shot multibox detector. In: *European conference on computer vision*. pp. 21–37. Springer (2016)
32. Liu, Y.C., Ma, C.Y., He, Z., Kuo, C.W., Chen, K., Zhang, P., Wu, B., Kira, Z., Vajda, P.: Unbiased teacher for semi-supervised object detection. *arXiv preprint arXiv:2102.09480* (2021)
33. Nassar, I., Herath, S., Abbasnejad, E., Buntine, W., Haffari, G.: All labels are not created equal: Enhancing semi-supervision via label grouping and co-training. In: *Proceedings of the IEEE/CVF Conference on Computer Vision and Pattern Recognition*. pp. 7241–7250 (2021)

34. Qiao, S., Shen, W., Zhang, Z., Wang, B., Yuille, A.: Deep co-training for semi-supervised image recognition. In: *Proceedings of the european conference on computer vision (eccv)*. pp. 135–152 (2018)
35. Redmon, J., Divvala, S., Girshick, R., Farhadi, A.: You only look once: Unified, real-time object detection. In: *Proceedings of the IEEE conference on computer vision and pattern recognition*. pp. 779–788 (2016)
36. Redmon, J., Farhadi, A.: Yolo9000: better, faster, stronger. In: *Proceedings of the IEEE conference on computer vision and pattern recognition*. pp. 7263–7271 (2017)
37. Ren, S., He, K., Girshick, R., Sun, J.: Faster r-cnn: Towards real-time object detection with region proposal networks. *Advances in neural information processing systems* **28** (2015)
38. Rezatofighi, H., Tsoi, N., Gwak, J., Sadeghian, A., Reid, I., Savarese, S.: Generalized intersection over union: A metric and a loss for bounding box regression. In: *Proceedings of the IEEE/CVF conference on computer vision and pattern recognition*. pp. 658–666 (2019)
39. Rizve, M.N., Duarte, K., Rawat, Y.S., Shah, M.: In defense of pseudo-labeling: An uncertainty-aware pseudo-label selection framework for semi-supervised learning. In: *International Conference on Learning Representations* (2021), <https://openreview.net/forum?id=-ODN6SbiUU>
40. Sohn, K., Berthelot, D., Li, C.L., Zhang, Z., Carlini, N., Cubuk, E.D., Kurakin, A., Zhang, H., Raffel, C.: Fixmatch: Simplifying semi-supervised learning with consistency and confidence. *arXiv preprint arXiv:2001.07685* (2020)
41. Sohn, K., Zhang, Z., Li, C.L., Zhang, H., Lee, C.Y., Pfister, T.: A simple semi-supervised learning framework for object detection. *arXiv preprint arXiv:2005.04757* (2020)
42. Tang, P., Ramaiah, C., Wang, Y., Xu, R., Xiong, C.: Proposal learning for semi-supervised object detection. In: *Proceedings of the IEEE/CVF Winter Conference on Applications of Computer Vision*. pp. 2291–2301 (2021)
43. Tang, Y., Chen, W., Luo, Y., Zhang, Y.: Humble teachers teach better students for semi-supervised object detection. In: *Proceedings of the IEEE/CVF Conference on Computer Vision and Pattern Recognition*. pp. 3132–3141 (2021)
44. Tarvainen, A., Valpola, H.: Mean teachers are better role models: Weight-averaged consistency targets improve semi-supervised deep learning results. *arXiv preprint arXiv:1703.01780* (2017)
45. Tian, Z., Shen, C., Chen, H., He, T.: Fcos: Fully convolutional one-stage object detection. In: *Proceedings of the IEEE/CVF international conference on computer vision*. pp. 9627–9636 (2019)
46. Wang, J., Chen, K., Yang, S., Loy, C.C., Lin, D.: Region proposal by guided anchoring. In: *Proceedings of the IEEE/CVF Conference on Computer Vision and Pattern Recognition*. pp. 2965–2974 (2019)
47. Wang, K., Zhang, L.: Reconcile prediction consistency for balanced object detection. In: *Proceedings of the IEEE/CVF International Conference on Computer Vision*. pp. 3631–3640 (2021)
48. Wang, Z., Li, Y., Guo, Y., Fang, L., Wang, S.: Data-uncertainty guided multi-phase learning for semi-supervised object detection. In: *Proceedings of the IEEE/CVF Conference on Computer Vision and Pattern Recognition*. pp. 4568–4577 (2021)
49. Xie, Q., Dai, Z., Hovy, E., Luong, M.T., Le, Q.V.: Unsupervised data augmentation for consistency training. *arXiv preprint arXiv:1904.12848* (2019)
50. Xie, Q., Luong, M.T., Hovy, E., Le, Q.V.: Self-training with noisy student improves imagenet classification. In: *Proceedings of the IEEE/CVF conference on computer vision and pattern recognition*. pp. 10687–10698 (2020)

51. Xu, M., Zhang, Z., Hu, H., Wang, J., Wang, L., Wei, F., Bai, X., Liu, Z.: End-to-end semi-supervised object detection with soft teacher. In: Proceedings of the IEEE/CVF International Conference on Computer Vision. pp. 3060–3069 (2021)
52. Yang, X., Wang, Y., Laganière, R.: A scale-aware yolo model for pedestrian detection. In: International Symposium on Visual Computing. pp. 15–26. Springer (2020)
53. Yang, X., Ye, J., Wang, X.: Factorizing knowledge in neural networks. arXiv preprint arXiv:2207.03337 (2022)
54. Zhang, B., Wang, Y., Hou, W., Wu, H., Wang, J., Okumura, M., Shinozaki, T.: Flexmatch: Boosting semi-supervised learning with curriculum pseudo labeling. *Advances in Neural Information Processing Systems* **34** (2021)
55. Zhang, F., Pan, T., Wang, B.: Semi-supervised object detection with adaptive class-rebalancing self-training. arXiv preprint arXiv:2107.05031 (2021)
56. Zhang, S., Chi, C., Yao, Y., Lei, Z., Li, S.Z.: Bridging the gap between anchor-based and anchor-free detection via adaptive training sample selection. In: CVPR (2020)
57. Zhang, X., Wan, F., Liu, C., Ji, R., Ye, Q.: Freeanchor: Learning to match anchors for visual object detection. *Advances in neural information processing systems* **32** (2019)
58. Zhang, Y., Yao, X., Liu, C., Chen, F., Song, X., Xing, T., Hu, R., Chai, H., Xu, P., Zhang, G.: S4od: Semi-supervised learning for single-stage object detection. arXiv preprint arXiv:2204.04492 (2022)
59. Zhou, Q., Yu, C., Wang, Z., Qian, Q., Li, H.: Instant-teaching: An end-to-end semi-supervised object detection framework. In: Proceedings of the IEEE/CVF Conference on Computer Vision and Pattern Recognition. pp. 4081–4090 (2021)
60. Zhu, B., Wang, J., Jiang, Z., Zong, F., Liu, S., Li, Z., Sun, J.: Autoassign: Differentiable label assignment for dense object detection. arXiv preprint arXiv:2007.03496 (2020)
61. Zhu, C., He, Y., Savvides, M.: Feature selective anchor-free module for single-shot object detection. In: Proceedings of the IEEE/CVF conference on computer vision and pattern recognition. pp. 840–849 (2019)
62. Zhu, X., Goldberg, A.B.: Introduction to semi-supervised learning. *Synthesis lectures on artificial intelligence and machine learning* **3**(1), 1–130 (2009)

In this supplementary material, we provide additional experimental quantitative results, model size comparison, as well as bounding boxes visualization further to support the effectiveness of our proposed **Consistent-Teacher**. In addition, we delineate more experimental details, implementation information, and hyper-parameter settings of our method. Our code is also attached for your reference.

## 1 More details of Consistent-Teacher

### 1.1 Balanced modality populations in Gaussian Mixture Model (GMM)

Although GMM is able to identify the two modalities in the distribution of confidence scores, there is also an imbalance in the populations of the positive and negative samples. For example, there could be only one positive prediction, while the rest are all negative samples. The substantial imbalance not only harms the convergence speed using Expectation-Maximization (EM) algorithm but may also result in imprecise thresholds between positive and negative modalities. In practice, we only put top- $K$  predictions into the score bank used to estimate a GMM model, where  $K = \text{round}(\sum_i^N b_i)$ , where  $b_i$  is the confidence score of a predicted bbox and  $N \sim 100$  is the number of total predictions from the teacher network. In this way, the population between positive and negative samples is more balanced and the GMM estimated threshold becomes more accurate.

### 1.2 Loss function

The loss function can be written as a general form

$$\mathcal{L} = \mathcal{L}_s + \lambda_u(\mathcal{L}_u^{cls} + \lambda^{reg}\mathcal{L}_u^{reg}), \quad (10)$$

where  $\mathcal{L}_s$  and  $\mathcal{L}_u$  denote supervised and unsupervised (unlabeled) losses, respectively.  $\lambda_u$  is the loss weight for  $\mathcal{L}_u$  and  $\lambda_{reg}$  is the loss weight for the regression subtask. In this study, GIoU loss [38] is used for regression, and parameters are set as  $\mathcal{L}_u = 2$  and  $\lambda_{reg} = 2$  across all different architectures. The standard Focal Loss [29] is adopted for classification in the MeanTeacher baseline that consists of an EMA-updated RetinaNet model, while the Focal loss [29] is used in **Consistent-Teacher** for better alignment between classification and regression tasks.

## 2 Semi-supervised detection results visualization

**Qualitative comparison with Baseline.** We further compare the baseline Mean Teacher RetinaNet with our **Consistent-Teacher** by visualizing the predicted bounding boxes on **val2017** under the COCO 10% protocol. In Figure 8, we plot the predicted and ground-truth bounding boxes in **Violet** and **Orange** respectively, alongside with the false positive bboxes highlighted in **Red**.

There are 3 general properties that we could observed in our demonstration.



1. First, **Consistent-Teacher** better fits the situation for crowded object localization, whereas Mean Teacher often mistakes the intersection of two overlapped objects as a new instance. For example, in scenes of zebras or sheep, Mean Teacher often gives a false positive output in the overlapping area of the two objects, where **Consistent-Teacher** largely resolved the inaccurate positioning problem through the adaptive anchor selection mechanism.
2. On the other hand, we see that under the semi-supervised setting, the Mean Teacher RetinaNet could either predict the wrong class for the correct location or regress inaccurate bounding boxes when the classification confidence is high. For example, birds are sometimes misidentified as airplanes even when the localization is accurate. It is mainly attributable to the inconsistency of classification and regression tasks, i.e. the features required for regression may not be optimal for classification. **Consistent-Teacher** effectively discriminates similar categories using the FAM-3D to select the features dynamically.
3. Third, **Consistent-Teacher** embraces higher recall since it is capable of detecting small or crowded instances where Mean Teacher fails to point out. For example, **Consistent-Teacher** finds most of the hot dogs on the grill while Mean Teacher neglects most of them.

**Good cases and Failure cases.** We provides more examples to showcase the good and failure examples produced by **Consistent-Teacher** on COCO val2017 in Figure 9 and Figure 10. Although our proposed method achieved gratifying performance on a series of SSOD benchmarks, we can still point out its deficiencies in Figure 10. First, the trained detector lacks robustness to some out-of-distribution samples, for example, cartoon characters on street signs are recognized as real people, and reflections in mirrors are recognized as objects. Second, our detection performance is poor for some classes with small sample size, such as toothbrushes, hair dryers, etc. Third, it also tends to treat parts of the object as a whole, such as the head of the giant panda as a separate individual (in the lower left corner), and the dial of a clock as the entire clock (on the right of the panda).

### 3 Experiment and Hyper-parameter settings

#### 3.1 Datasets and data preprocessing.

**MS-COCO 2017.** The Microsoft Common Objects in Context (MS-COCO) is a large-scale object detection, segmentation, key-point detection, and captioning dataset. We includes COCO2017 in our experiments for SSOD, which includes 118K/5K training validation images along with bounding boxes with 80 object categories.

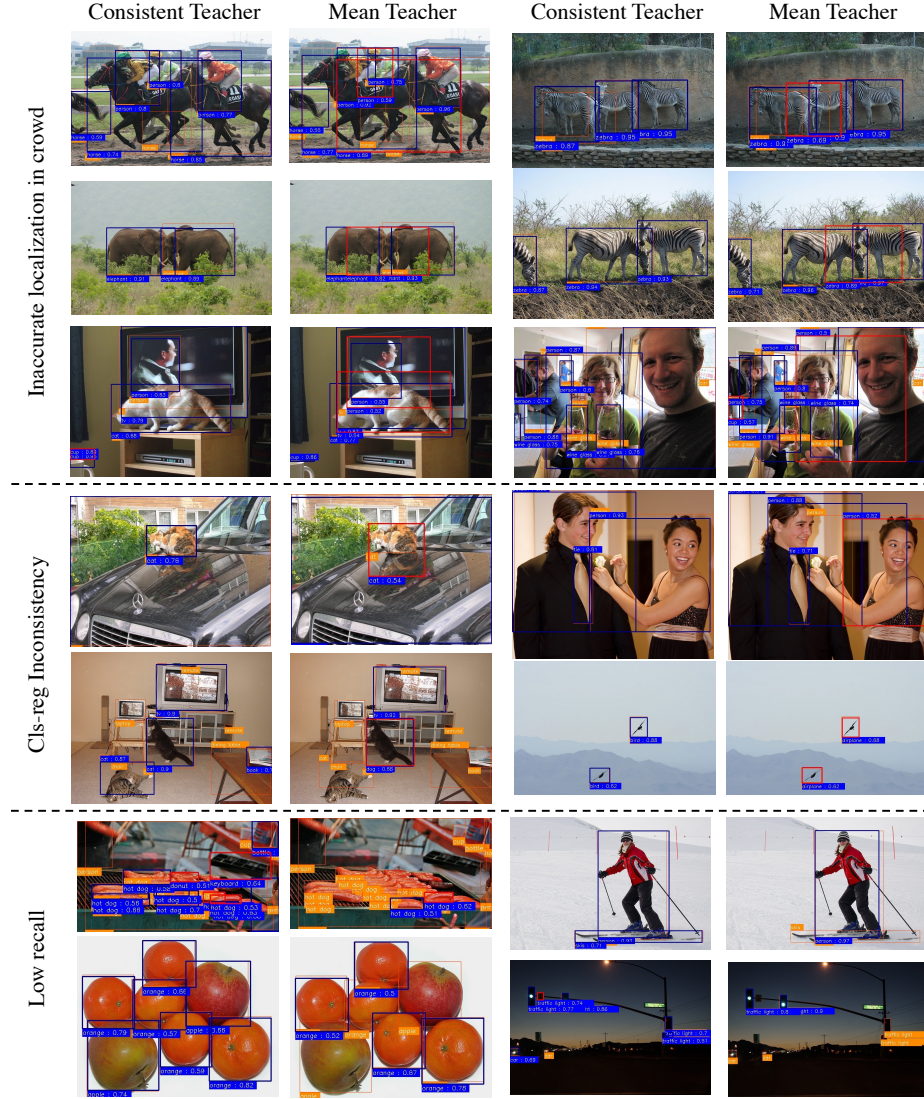


**Fig. 8.** Qualitative comparison on the COCO%10 evaluation. The bounding boxes in Orange is the ground-truth, and Violet refers to the prediction. Red highlights the false positive predictions.

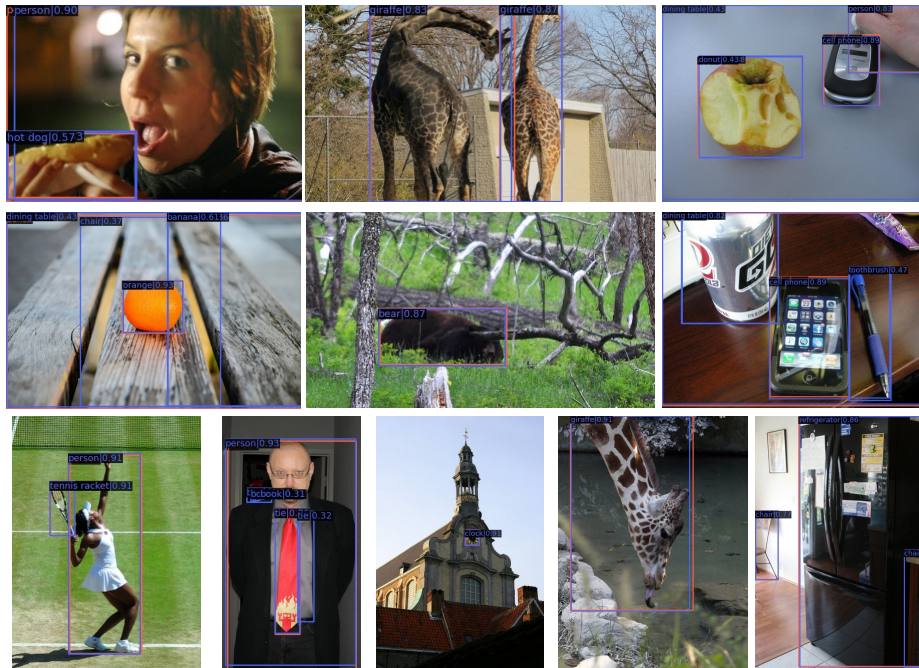


**Fig. 9.** Good detection results for the COCO%10 evaluation. The bounding boxes in Orange is the ground-truth, and Violet refers to the prediction.

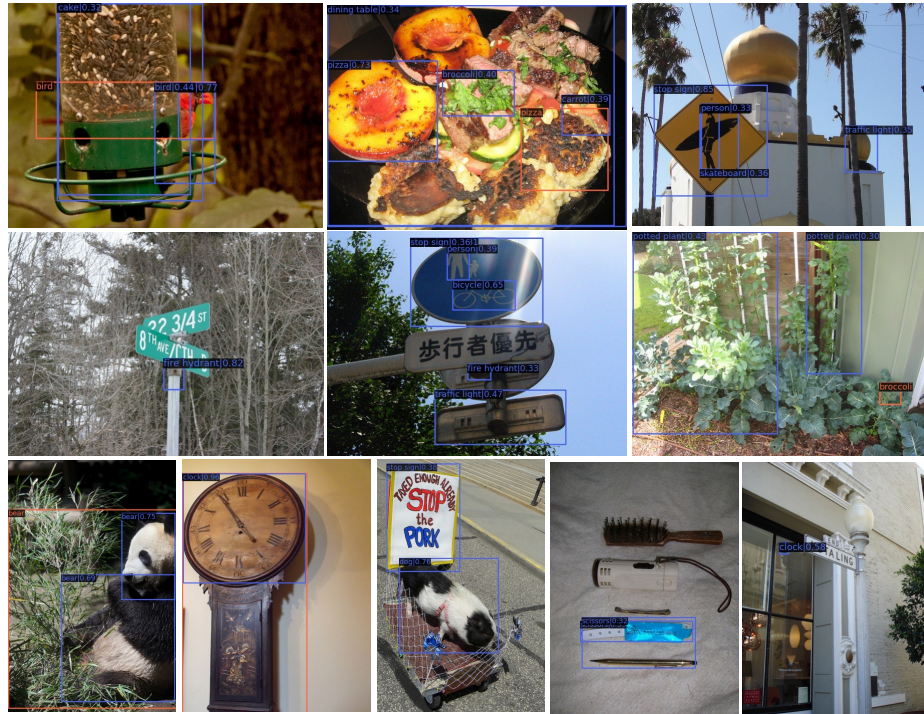


**Fig. 10.** Failure detection results for the COCO%10 evaluation. The bounding boxes in **Orange** is the ground-truth, and **Violet** refers to the prediction.

**PASCAL VOC 2007-2012.** The PASCAL Visual Object Classes (VOC) dataset contains 20 object categories alongside with pixel-level segmentation annotations, bounding box annotations, and object class annotations. The official VOC 2007 `trainval` set is adopted as the labeled set with 5011 images and the 11540 images from VOC 2012 `trainval` set is the unlabeled data. We evaluate on the VOC 2007 test set.

**Data Augmentations.** We use the same data augmentations as described in Soft Teacher [51], including a labeled data augmentation in Table 9, a weak unlabeled augmentation in Table 10 and a strong unlabeled augmentation in Table 11.

### 3.2 Implementation Details

We implement our **Consistent-Teacher** based on MMDetection<sup>5</sup> framework, as the data preprocessing code borrowed from open-sourced Soft-Teacher<sup>6</sup> and google ssl-detection<sup>7</sup>. We train our detectors on 8 NVIDIA Tesla V100 GPUs. It takes approximately 3 days for a 180K training. Each GPU contains 1 labeled image a and 4 unlabeled images. The source code is attached in the a separate zip file.

---

<sup>5</sup> <https://github.com/open-mmlab/mmdetection>

<sup>6</sup> <https://github.com/microsoft/SoftTeacher>

<sup>7</sup> [https://github.com/google-research/ssl\\_detection/](https://github.com/google-research/ssl_detection/)

**Table 9.** Data augmentation for labeled image training.

Transformation	Description	Parameter Setting
RandomResize	Resize the image to a the height of $h$ randomly sampled from $h \sim U(h_{min}, h_{max})$ , while keeping the height-width ratio unchanged.	$h_{min} = 400, h_{max} = 1200$ in MS-COCO $h_{min} = 480, h_{max} = 800$ in PASCAL-VOC
RandomFlip	Randomly horizontally flip a image with probability of $p$ .	$p = 0.5$
OneOf	Select one of the transformation in a transformation set $T$ .	$T = \text{TransAppearance}$

**Table 10.** Weak data augmentation for unlabeled image.

Transformation	Description	Parameter Setting
RandomResize	Resize the image to a the height of $h$ randomly sampled from $h \sim U(h_{min}, h_{max})$ , while keeping the height-width ratio unchanged.	$h_{min} = 400, h_{max} = 1200$ in MS-COCO $h_{min} = 480, h_{max} = 800$ in PASCAL-VOC
RandomFlip	Randomly horizontally flip a image with probability of $p$ .	$p = 0.5$

**Table 11.** Strong data augmentation for unlabeled image.

Transformation	Description	Parameter Setting
RandomResize	Resize the image to a the height of $h$ randomly sampled from $h \sim U(h_{min}, h_{max})$ , while keeping the height-width ratio unchanged.	$h_{min} = 400, h_{max} = 1200$ in MS-COCO $h_{min} = 480, h_{max} = 800$ in PASCAL-VOC
RandomFlip	Randomly horizontally flip a image with probability of $p$ .	$p = 0.5$
OneOf	Select one of the transformation in a transformation set $T$ .	$T = \text{TransAppearance}$
OneOf	Select one of the transformation in a transformation set $T$ .	$T = \text{TransGeo}$
RandErase	Randomly selects $K$ rectangle region of size $\lambda h \times \lambda w$ in an image and erases its pixels with random values, where $(h, w)$ are height and width of the original image.	$K \in U(1, 5)$ $\lambda \in U(0, 0.2)$



**Table 12.** Appearance transformations, called **TransAppearance**.

Transformation	Description	Parameter Setting
Identity	Returns the original image.	
Autocontrast	Maximizes the image contrast by setting the darkest (lightest) pixel to black (white).	
Equalize	Equalizes the image histogram.	
RandSolarize	Invert all pixels above a threshold value $T$ .	$T \in U(0, 1)$
RandColor	Adjust the color balance of image. $C = 0$ returns a black&white image, $C = 1$ returns the original image.	$C \in U(0.05, 0.95)$
RandContrast	Adjust the contrast of image. $C = 0$ returns a solid grey image, $C = 1$ returns the original image.	$C \in U(0.05, 0.95)$
RandBrightness	Adjust the brightness of image. $C = 0$ returns a black image, $C = 1$ returns the original image.	$C \in U(0.05, 0.95)$
RandSharpness	Adjust the sharpness of image. $C = 0$ returns a blurred image, $C = 1$ returns the original image.	$C \in U(0.05, 0.95)$
RandPolarize	Reduce each pixel to $C$ bits.	$C \in U(4, 8)$

**Table 13.** Geometric transformations, called **TransGeo**.

Transformation	Description	Parameter Setting
RandTranslate X	Translate the image horizontally by $\lambda \times$ image width.	$\lambda \in U(-0.1, 0.1)$
RandTranslate Y	Translate the image vertically by $\lambda \times$ image height.	$\lambda \in U(-0.1, 0.1)$
RandRotate Y	Rotates the image by $\theta$ degrees.	$\theta \in U(-30^\circ, 30^\circ)$
RanShear X	Shears the image along the horizontal axis with rate $R$ .	$R \in U(-0.480, 0.480)$
RanShear Y	Shears the image along the vertically axis with rate $R$ .	$R \in U(-0.480, 0.480)$